PHASE CHANGE HEAT TRANSFER CHARACTERISTICS OF WATER/PAO NANOEMULSION HEAT TTRANSFER FLUIDS

Jiajun Xu
jiajun.xu@udc.edu
University of the District of Columbia
4200 Connecticut Ave, NW,DC,20008

Abstract

In this study, one type of nano-engineered heat transfer fluids: Water/AOT/Polyalphaolefin (PAO) nanoemulsion fluids are prepared, and their phase change heat transfer properties have been investigated. The Water/AOT/Polyalphaolefin nanoemulsion heat transfer fluids which are thermodynamically stable are spontaneously generated by a self-assembly of dispersed water nanodroplets

The results, expressed in terms of surface heat flux as the function of temperature, have shown that liquid-vapor phase change of water nanodroplets has a drastic impact on the boiling behavior of the nanoemulsion fluid studied: the adding of water nanodroplets greatly lowers the nanoemulsion's boiling point compared to base polyalphaolefin oil while its heat transfer coefficient increases by over 300% after the incipience of boiling. Meanwhile, the addition of water nanodroplets has greatly enhanced the effective specific heat of the base polyalphaolefin oil by over 70% while undergoing liquid-solid phase change.

Besides that, the pool boiling trend of these nanoemulsion heat transfer fluids randomly follows two different boiling curves which coincides with the water inner structure variation based on Small Angle Neutron Scattering (SANS) measurement.

Key words: Phase change, Heat transfer, nanoemulsion, small angle neutron scattering

Introduction

Phase change heat transfer is a complex but very useful phenomenon widely used in industry and military areas [1-19]. Conventional coolants, lubricants and other heat transfer fluids used in today's thermal systems typically have relatively poor heat transfer properties. Hence, utilizing the phase change process to increase the heat transfer properties of conventional fluids is another promising direction. Recently, the author has proposed a new "nanoemulsion heat transfer fluid" system in which one lower boiling point liquid is dispersed into another immiscible liquid as self-assembled nanodroplets to improve the fluid thermal properties especially its phase change characteristics[9-12, 15, 17]. The nanoemulsion heat transfer fluids belong to the family of microemulsion and are thermodynamically stable.

In this paper, the phase change heat transfer characteristics of water-in-PAO nanoemulsion fluids, especially their liquid-to-gas and liquid-to-solid phase change properties, have been investigated experimentally.

EXPERIMENTAL RESULTS AND DISCUSSION

The water-in-PAO nanoemulsion fluids are spontaneously generated by self-assembly. These water nanodroplets are reverse micelles swollen with water, and stabilized by the surfactant molecules AOT (Sigma Aldrich) that have hydrophilic heads facing inward and hydrophobic tails facing outward into the base fluid PAO 2cst (Chevron Philips Chemical Company). The water-in-PAO nanoemulsion fluids are transparent, but scatter light due to the Tyndall effect, as shown in Figure 1.

The liquid-to-gas phase change properties for the nanoemulsion fluids with water are measured using pool boiling test rig and the heat transfer capability with water concentrations are plotted in Figure 2 and 3. As shown in Figures 2 and 3, all tested water-in-PAO nanoemulsion fluids start to boil at around 170 ^{o}C. At low heat flux levels, single-phase natural convection appears to the same for the nanoemulsion fluids and the pure PAO. This indicates that without phase transition, these water nanodroplets have insignificant effect on the fluid heat transfer. At sufficiently large wall superheat (about 70^{o}C), nucleate boiling begins on the heater surface in these nanoemulsion fluids. The curves after boiling incipience have a similar slope and appear to coincide for the water-in-PAO nanoemulsion fluids with different water concentrations. But the critical heat flux decreases with the increasing water nanodroplet loading[20, 21].

The curves after boiling incipience may fall into two different curves depending on the water concentration. For those with water volume concentrations less than 4.5% (like the 1.8% and 3.6% shown in Figure 2), they have a similar slope and they coincide with each other until reaching CHF which decreases with higher water loading.

However, for those of water concentrations from 5.3 Vol% to 7.8 Vol%, the CHF varies by randomly falling into two different boiling curves as shown in Figure 3. One boiling curve has a lower critical heat flux, but the wire burns out after the critical heat flux is reached, without experiencing transition and film boiling. This type of curve is called 1st curve and plotted with red colored symbols in the Figure 3. In the second type of curves, the critical heat flux is higher for the same water concentration, and the wire burnout occurs in the film boiling regime. Those

data plotted in Figure 3 with blue colored symbols represent the second type of curve for the nanoemulsion of the same water loading (7.8 Vol%). If the water content is above 8.6%, the wire burnout always occurs in the film boiling regime as shown in figure 3 with black colored symbols. It is also observed experimentally that the probability of the occurrence of the 1st boiling curve decreases with increasing water loading.

The observed random behavior of the nanoemulsion boiling also coincides with the dynamics and microstructure within the nanoemulsion fluids. Figure 4 shows the Small Angle Neutron Scattering(SANS) data for water-in-PAO nanoemulsion fluids with water volumetric concentration covering 1.8 Vol% to 10.3 Vol%. Two empirical fittings are used to find out the inner structure.[22-25]

Figure 4 shows the processed SANS data for water volumetric concentrations covering 1.8 Vol% to 10.3 Vol%. The scattering intensity I varies with the scattering vector $q = 4\pi \sin(\theta/2)/\lambda$, where λ is the wavelength of the incident neutrons, and θ is the scattering angle. The approximation $q = 2\pi\theta/\lambda$ is used for SANS (due to the small-angle θ). It can be seen in this figure that the neutron scattering curves fall in to two different groups: for water loading of 1.8~4.5 %, the curves level off when the scattering intensity q is less than 0.1 A^{-1}. In contrast, the curves have a downward sloping shape for water loading of 5.3%~7.8 % while the curves shift to a more obvious ternary form for water loading of 8.6% and 10.3%. The different groups are marked using three different colors as shown in Figure 4.

The fitting of SANS data were processed using the IGOR Pro software under the protocol from NCNR NIST and plotted in Figure 4 [17, 23, 26, 27]. The hard sphere model fits well for low water concentration curves (i.e. 1.8~4.5 vol.%), and the nanodroplet radii are found to be 13.2$\dot{A}$, 25.6$\dot{A}$ and 96$\dot{A}$ for water loading 1.8 vol.%, 3.6 vol.% and 4.5 vol. %, respectively. For higher water concentration (i.e. 7.8 ~10.3 vol.%), the hard-sphere model doesn't fit well especially for scattering q less than 0.1 A^{-1} region, which suggests that those nanodroplets are not simply spherical. The 3-region Guinier-Porod empirical model is used to determine the nanodroplet geometry by fitting the SANS data. According to the 3-region Guinier-Porod model[27], there are two dimensionality parameter S_1 and S_2, and plus R_{g2} and $R_{g1}$are the radii of gyration for the short and overall sizes of the scattering object. The fitted curves give $S_2 = 0.22$, $S_1 = 1.4$ and $R_{g2} = 121\dot{A}, R_{g1} = 4.6\dot{A}$ for 10.3 Vol.% sample. For 7.8 Vol.% one, $S_2 = 0.18, S_1 = 0.97$ and $R_{g2} = 47.4\dot{A}, R_{g1} = 5.2\dot{A}$. The dimensionality parameters suggest that those nanodroplets have a cylinder-like shape[27].

From the aforementioned analysis, it can be assessed that that the nanodroplet size and shape depend on water concentration in Water-PAO nanoemulsion fluids. The water nanodroplets change from sphere to elongated cylinder when the water concentration increases, especially above 5.3 vol. %. Interestingly, this change in droplet shape coincides with the change in fluid viscosity and pooling boiling behavior. No satisfactory explanation to this observed structure-property relation is currently available since the mechanisms of nanoemulsion fluids' boiling are little known.

Meanwhile, another important liquid-to-solid phase change property: the heat capacity of water-in-PAO nanoemulsion fluids is also investigated. Theoretically, the heat capacity can be enhanced through two different mechanisms: one is due to the high specific heat of the dispersed phase; the other is due to the latent heat of the dispersed phase changeable nanodroplets[13, 28-

30]. The latter one, i.e., use of phase changeable nanodroplets, is much more efficient for the heat capacity enhancement. In water in PAO nanoemulsion fluids, the fluid's heat capacity can be increased by the high specific heat of water (i.e., C_{water}=4.2 J/g C, C_{PAO}=1.88 J/g C) or the latent heat of water ($\Delta H = 334$ J/g), depending on the operating temperature of the fluids.

The specific heat of the pure PAO and water in PAO nanoemulsion fluids are measured using a Differential Scanning Calorimetry (DSC).[12, 31, 32] DSC is a thermoanalytical technique that has been widely used to measure the latent heat of phase change materials. In this method, both the sample and reference are maintained at nearly the same temperature by adjusting heat input to them. The difference in the amount of heat supplied to the sample and the reference is recorded as a function of temperature (or time). In the curve of heat flux versus temperature or versus time, a positive or negative peak corresponds to exothermic or endothermic reactions in the sample, respectively. Enthalpies of phase transitions can be calculated by integrating the peak corresponding to a given transition, $\Delta H = c \cdot A$ where A is the area of the peak and c is the calorimetric constant. In order to determine the sample heat capacity, three measurements are usually carried out: the sample, the baseline and a standard. The baseline is subtracted from the sample record to obtain absolute values of the heat flow to the sample. The heat capacity can be determined by the heat flow, the temperature rise and the sample mass.

During the heating and cooling cycle, water nanodroplets undergo melting-freezing transition in the nanoemulsion fluids. The peak at about -20 ℃ is the exothermic crystallization (freezing) peak for the water nanodroplets in the fluids. These water nanodroplets exhibit a relatively large melting-freezing hysteresis, about 20 ℃. On the other hand, the presence of a single freezing peak in Figure 5 indicates that the nanoemulsion fluids are well dispersed and all water nanodroplets are nearly monodispersed in size which agrees well with our SANS measurement result.

The impact of phase-changeable water nanodroplets on the fluid properties is obvious: the effective specific heat of the fluids can be significantly boosted. The effective specific heat can be defined as $C_{nanoemulsion} = C_{base\_fluid} + \phi H_{f,droplet} / \Delta T$, where ϕ is the volume fraction of the phase-changeable nanodroplets, $H_{f,droplet}$ is the latent heat of the phase-changeable nanodroplets per unit volume, and ΔT is the temperature difference between the heat transfer surface and the bulk fluid. In this experiment, if assuming ΔT =20 ℃, the effective volumetric specific heat can be increased by up to 70% for the nanoemulsion fluid containing 8 vol % water nanodroplets when the water nanodroplets undergo phase transition. So the usage of phase-changeable water nanodroplets provides a way to simultaneously increase the effective specific heat and heat transfer coefficient of conventional heat transfer fluids.

In summary, both liquid-to-gas and liquid-to-solid phase change properties of the water-in-PAO nanoemulsion fluids have been investigated under different water concentrations. The pool boiling characteristics are highly dependent upon the water volumetric concentration which can randomly follow two different types of curves when the water concentrations are in the range of 5.3 Vol. % to 7.8 Vol. %. This could be attributed to the dynamics and microstructure of the nanoemulsion fluids, however, more study is needed to further clarify the mechanism behind Meanwhile, the addition of phase changeable water nanodroplets can also greatly enhance the effective heat capacity of the nanoemulsion fluids by upto 70%.

REFERENCES

[1] Eastman, L. J., Choi, S. U. S., LI, S., and Thompson, L. J., 1997, "*Enhanced thermal conductivity through development of nanofluids*,"Nanocrystalline and Nanocomposite Materials II.

[2] Eastman, J. A., Choi, S. U. S., Li, S., Yu, W., and Thompson, L. J., 2001, "*Anomalously increased effective thermal conductivities of ethylene glycol-based nanofluids containing copper nanoparticles*," Applied Physics Letters, 78(6), pp. 718-720.

[3] Choi, S. U. S., Zhang, Z. G., Yu, W., Lockwood, F. E., and Grulke, E. A., 2001, "*Anomalous thermal conductivity enhancement in nanotube suspensions*," Applied Physics Letters, 79(14), pp. 2252-2254.

[4] You, S. M., Kim, J. H., and Kim, K. H., 2003, "*Effect of nanoparticles on critical heat flux of water in pool boiling heat transfer*," Applied Physics Letters, 83(16), pp. 3374-3376.

[5] Wen, D. S., and Ding, Y. L., 2004, "*Effective thermal conductivity of aqueous suspensions of carbon nanotubes (carbon nanotubes nanofluids)*," Journal of Thermophysics and Heat Transfer, 18(4), pp. 481-485.

[6] Li, C. H., and Peterson, G. P., 2006, "*Experimental investigation of temperature and volume fraction variations on the effective thermal conductivity of nanoparticle suspensions (nanofluids)*," Journal of Applied Physics, 99(8).

[7] Prasher, R., Evans, W., Meakin, P., Fish, J., Phelan, P., and Keblinski, P., 2006, "*Effect of aggregation on thermal conduction in colloidal nanofluids*," Applied Physics Letters, 89(14).

[8] Yang, S. H., Baek, W. P., and Chang, S. H., 1997, "*Pool-boiling critical heat flux of water on small plates: Effects of surface orientation and size*," International Communications in Heat and Mass Transfer, 24(8), pp. 1093-1102.

[9] Yang, B., Liu, W. L., Liu, J. L., Wang, K. L., and Chen, G., 2002, "*Measurements of anisotropic thermoelectric properties in superlattices*," Applied Physics Letters, 81(19), pp. 3588-3590.

[10] Yang, B., and Han, Z. H., 2006, "*Thermal conductivity enhancement in water-in-FC72 nanoemulsion fluids*," Applied Physics Letters, 88(26).

[11] Yang, B., and Han, Z. H., 2006, "*Temperature-dependent thermal conductivity of nanorod-based nanofluids*," Applied Physics Letters, 89(8).

[12] Han, Z. H., and Yang, B., 2008, "*Thermophysical characteristics of water-in-FC72 nanoemulsion fluids*," Applied Physics Letters, 92(1).

[13] Yang, B., 2008, "*Thermal conductivity equations based on Brownian motion in suspensions of nanoparticles (nanofluids)*," Journal of Heat Transfer-Transactions of the Asme, 130(4).

[14] Buongiorno, J., Venerus, D. C., Prabhat, N., McKrell, T., Townsend, J., Christianson, R., Tolmachev, Y. V., Keblinski, P., Hu, L.-w., Alvarado, J. L., Bang, I. C., Bishnoi, S. W., Bonetti, M., Botz, F., Cecere, A., Chang, Y., Chen, G., Chen, H., Chung, S. J., Chyu, M. K., Das, S. K., Di Paola, R., Ding, Y., Dubois, F., Dzido, G., Eapen, J., Escher, W., Funfschilling, D., Galand, Q., Gao, J., Gharagozloo, P. E., Goodson, K. E., Gutierrez, J. G., Hong, H., Horton, M., Hwang, K. S., Iorio, C. S., Jang, S. P., Jarzebski, A. B., Jiang, Y., Jin, L., Kabelac, S., Kamath, A., Kedzierski, M. A., Kieng, L. G., Kim, C., Kim, J.-H., Kim, S., Lee, S. H., Leong, K. C., Manna, I., Michel, B., Ni, R., Patel, H. E., Philip, J., Poulikakos, D., Reynaud, C., Savino, R., Singh, P. K., Song, P., Sundararajan, T., Timofeeva, E., Tritcak, T., Turanov, A. N., Van Vaerenbergh, S., Wen, D., Witharana, S., Yang, C., Yeh, W.-H., Zhao, X.-Z., and Zhou, S.-Q., 2009, "*A benchmark study on the thermal conductivity of nanofluids*," Journal of Applied Physics, 106(9).

[15] Xu, J. J., Wu, C. W., and Yang, B., 2010, "*Thermal- and Phase-Change Characteristics of Self-Assembled Ethanol/Polyalphaolefin Nanoemulsion Fluids*," Journal of Thermophysics and Heat Transfer, 24(1), pp. 208-211.

[16] Wu, C., Cho, T. J., Xu, J., Lee, D., Yang, B., and Zachariah, M. R., 2010, "*Effect of nanoparticle clustering on the effective thermal conductivity of concentrated silica colloids*," Physical Review E, 81(1).

[17] Xu, J., Yang, B., and Hammouda, B., 2011, "*Thermal conductivity and viscosity of self-assembled alcohol/polyalphaolefin nanoemulsion fluids*," Nanoscale Research Letters, 6.

[18] Henry, C. D., and Kim, J. H., 2004, "*A study of the effects of heater size, subcooling, and gravity level on pool boiling heat transfer*," International Journal of Heat and Fluid Flow, 25(2), pp. 262-273.

[19] Kim, J. B., Oh, B. D., and Kim, M. H., 2006, "*Experimental study of pool temperature effects on nucleate pool boiling*," International Journal of Multiphase Flow, 32(2), pp. 208-231.

[20] Hodgson, A. S., 1969, "*HYSTERESIS EFFECTS IN SURFACE BOILING OF WATER*," Journal of Heat Transfer, 91(1), pp. 160-&.

[21] Celata, G. P., Cumo, M., and Setaro, T., 1992, "*HYSTERESIS PHENOMENA IN SUBCOOLED FLOW BOILING OF WELL-WETTING FLUIDS*," Experimental Heat Transfer, 5(4), pp. 253-275.

[22] Gradzielski, M., and Langevin, D., 1996, "*Small-angle neutron scattering experiments on microemulsion droplets: Relation to the bending elasticity of the amphiphilic film*," Journal of Molecular Structure, 383(1-3), pp. 145-156.
[23] Hammouda, B., 2010, "*SANS from Polymers-Review of the Recent Literature*," Polymer Reviews, 50(1), pp. 14-39.
[24] Lisy, V., and Brutovsky, B., 2000, "*Interpretation of static and dynamic neutron and light scattering from microemulsion droplets: Effects of shape fluctuations*," Physical Review E, 61(4), pp. 4045-4053.
[25] Marszalek, J., Pojman, J. A., and Page, K. A., 2008, "*Neutron Scattering Study of the Structural Change Induced by Photopolymerization of AOT/D(2)O/Dodecyl Acrylate Inverse Microemulsions*," Langmuir, 24(23), pp. 13694-13700.
[26] Hammouda, B., Krueger, S., and Glinka, C. J., 1993, "*SMALL-ANGLE NEUTRON-SCATTERING AT THE NATIONAL-INSTITUTE-OF-STANDARDS-AND-TECHNOLOGY*," Journal of Research of the National Institute of Standards and Technology, 98(1), pp. 31-46.
[27] Hammouda, B., 2010, "*A new Guinier-Porod model*," Journal of Applied Crystallography, 43, pp. 716-719.
[28] Moulik, S. P., Das, M. L., Bhattacharya, P. K., and Das, A. R., 1992, "*THERMODYNAMICS OF MICROEMULSION FORMATION .1. ENTHALPY OF SOLUTION OF WATER IN BINARY (TRITON-X 100 + BUTANOL) AND TERNARY (HEPTANE + TRITON-X 100 + BUTANOL) MIXTURES AND HEAT-CAPACITY OF THE RESULTING SYSTEMS*," Langmuir, 8(9), pp. 2135-2139.
[29] Mulligan, J. C., Colvin, D. P., and Bryant, Y. G., 1996, "*Microencapsulated phase-change material suspensions for heat transfer in spacecraft thermal systems*," Journal of Spacecraft and Rockets, 33(2), pp. 278-284.
[30] Ray, S., Bisal, S. R., and Moulik, S. P., 1994, "*THERMODYNAMICS OF MICROEMULSION FORMATION .2. ENTHALPY OF SOLUTION OF WATER IN BINARY-MIXTURES OF AEROSOL-OT AND HEPTANE AND HEAT-CAPACITY OF THE RESULTING SYSTEMS*," Langmuir, 10(8), pp. 2507-2510.
[31] Han, Z. H., Cao, F. Y., and Yang, B., 2008, "*Synthesis and thermal characterization of phase-changeable indium/polyalphaolefin nanofluids*," Applied Physics Letters, 92(24).
[32] Han, Z. H., Yang, B., Qi, Y., and Cumings, J., 2011, "*Synthesis of low-melting-point metallic nanoparticles with an ultrasonic nanoemulsion method*," Ultrasonics, 51(4), pp. 485-488.

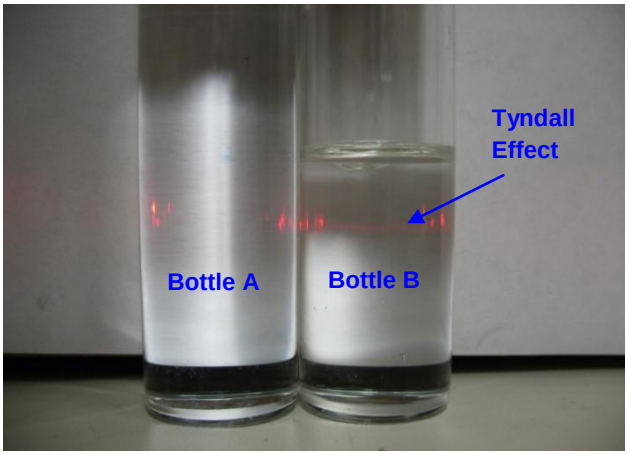

Figure 1. Water-in-PAO nanoemulsion fluid (Bottle A) and pure PAO (Bottle B). The Tyndall effect shown in figure 1 is used to distinguish each other.

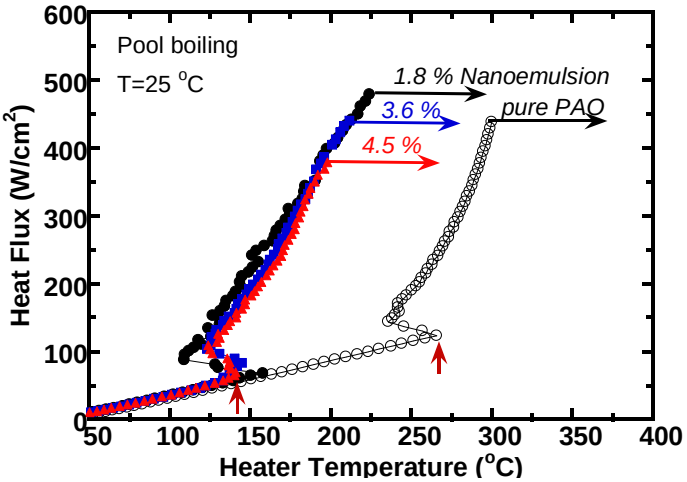

Figure 2. Pool boiling curves for Water in PAO nanoemulsion fluids: water volume fraction from 1.8% to 4.5%. The arrows in the figure represent where the burn out of wire occurs.

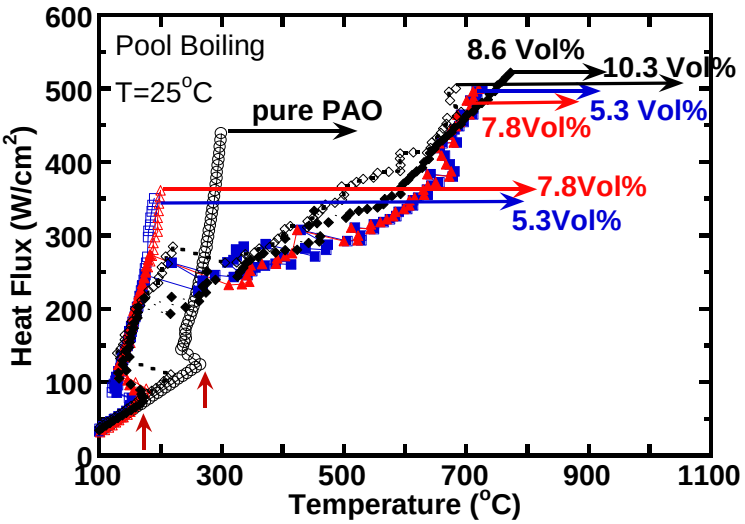

Figure 3. Pool boiling curves for Water in PAO nanoemulsion fluids: water volume fraction from 5.3% to 10.3%.

The arrows in the figure represent where the burn out of wire occurs.

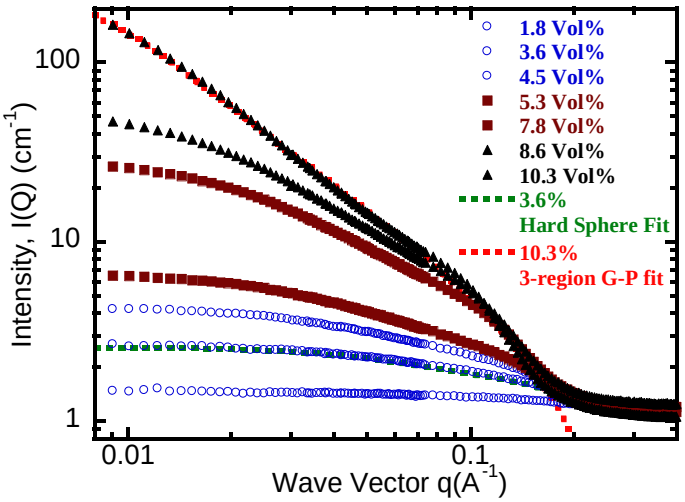

Figure. 4: SANS scattering curve Intensity I vs Wave Vector q with curve fitting

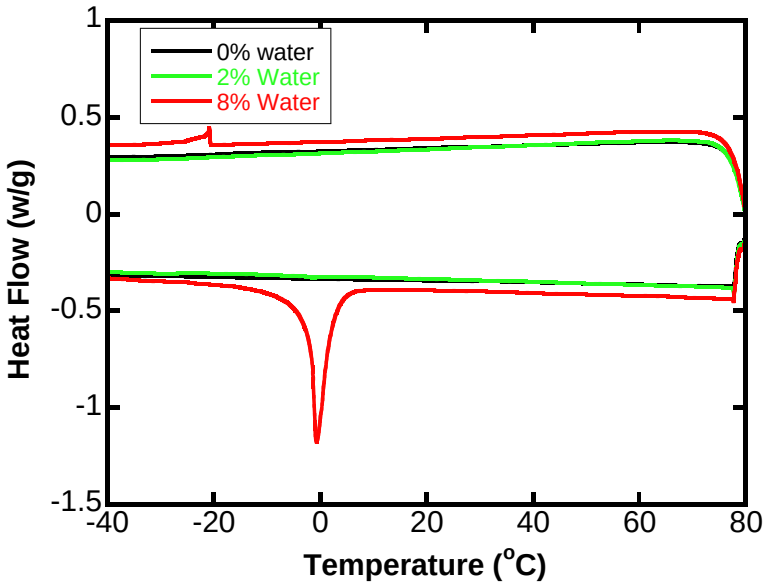

Figure 5 DSC cyclic curves of water-in-PAO nanoemulsions for different water concentrations.